(center, 4 H, AA'BB', CH_2CH_2); ^{13}C NMR ($CDCl_3$) δ 274.5 (μ-CO), 212.2 (CO), 158.5 (μ-C, quintet, J_{C-C-H} = 4.5 Hz), 90.3 (C_5H_5, doublet of quintets, J_{C-H} = 178.5 Hz, J_{C-C-H} = $J_{C-C-C-H}$ = 6.7 Hz), 22.2 (CH_2CH_2, triplet of triplets, J_{C-H} = 159.1 Hz, J_{C-C-H} = 4.1 Hz), MS (70 eV), m/e 366 (M^+), 338 (M^+ – CO), 310 (M^+ – 2CO), 282 (M^+ – 3CO), 242 (M^+ – 3CO – C_3H_4). Anal. Calcd for $C_{16}H_{14}O_3Fe_2$: C, 52.51; H, 3.86; Fe, 30.52. Found: C, 52.30; H, 3.97; Fe, 29.89.

***cis*-(η^5-C_5H_5)$_2$Fe$_2$(CO)$_2$(μ-CO)(μ-$\overline{CCH_2CH_2}$) (2c).** A total of 165 mL of CH_2N_2 in ether (0.19 M, 11.2 equiv) was added dropwise with vigorious stirring to a slurry of **1c** (1.00 g, 2.8 mmol) and CuCl (0.5 g, 5 mmol) in ether (15 mL). The mixture was filtered and the ether solution concentrated to yield 836 mg (80%) of red crystalline **2c**: mp 161–162 °C dec; IR (hexane) 1996 (vs), 1961 (m), 1802 (s) cm^{-1}; ^1H NMR (acetone-d_6) δ 4.76 (10 H, s, Cp), 2.05, 1.52 (4 H, AA'XX', $J_{AA'}$ = –8.1 Hz, $J_{XX'}$ = –7.6 Hz, J_{AX}(cis) = 10.4 Hz, $J_{AX'}$(trans) = 5.7 Hz, CH_2CH_2); ^{13}C NMR ($CDCl_3$) δ 273.5 (μ-CO), 212.4 (CO), 155.8 (μ-C, quintet, J_{C-C-H} = 4.5 Hz), 88.3 (C_5H_5 doublet of quintets, J_{C-H} = 177.9 Hz, J_{C-C-H} = $J_{C-C-C-H}$ = 6.6 Hz), 22.3 (CH_2, triplet of triplets, J_{C-H} = 157 Hz, J_{C-C-H} = 2.5 Hz), 21.6 (CH_2, triplet of triplets, J_{C-H} = 158 Hz, J_{C-C-H} = 2.5 Hz); MS (70 eV), m/e 366 (M^+), 338 (M^+ – CO), 310 (M^+ – 2CO), 282 (M^+ – 3CO), 242 (M^+ – 3CO – C_3H_4). Anal. Calcd for $C_{16}H_{14}O_3Fe_2$: C, 52.51; H, 3.86; Fe, 30.52. Found: C, 52.69; H, 3.93; Fe, 30.75.

X-ray Analysis. The complex crystallizes from ether as red prisms. Diffraction data were collected on a crystal of dimensions 0.40 mm × 0.30 mm × 0.20 mm. A summary of crystallographic data and the experimental conditions are given in Table I. Diffraction data were collected on an Enraf-Nonius CAD-4 diffractometer and were corrected for absorption (μ = 20.2 cm^{-1}, empirical ψ scan technique). All calculations were performed by using the SDP package provided by Enraf-Nonius. The iron atoms were located by inspection of a three-dimensional Patterson function and the remaining non-hydrogen atoms by least-squares structure factor calculations and difference Fourier techniques. Positions of the hydrogen atoms were then found by a combination of difference Fourier techniques and the use of HYDRO from the SDP package. The hydrogen positions were not refined. All non-hydrogen positions were then refined with anisotropic thermal parameters. Least-squares refinement converged with residuals of R = 0.032, R_w = 0.037, using 446 data with $I > 3\sigma(I)$ from 2θ(Mo Kα) = 0–25°, the esd of an observation of unit weight was 1.091.

Acknowledgment. We gratefully acknowledge R. M. Lach and E. G. Habeeb for their assistance in the syntheses described herein and Drs. K. D. Rose and C. S. Hsu of the Analytical Division of Exxon Research and Engineering Co. for the NMR and mass spectra reported.

Registry No. **1c**, 86420-26-0; **1t**, 86420-25-9; **2c**, 91547-48-7; **2t**, 91443-97-9; CH_2N_2, 334-88-3.

Supplementary Material Available: Tables listing least-squares planes and deviations (Table V), dihedral angles between the planes (Table VI), anisotropic thermal parameters (Table VII), and observed and calculated structure factor amplitudes (Table VIII) (6 pages). Ordering information is given on any current masthead page.

Syntheses, Molecular Structures, and Stabilities of Binuclear Complexes [$Pt_2Me_4(\mu$-$R_2PCH_2PR_2)_2$]

Ljubica Manojlović-Muir,*[1a] Kenneth W. Muir,[1a] Aileen A. Frew,[1a] Samson S. M. Ling,[1b] Mary A. Thomson,[1b] and Richard J. Puddephatt*[1b]

Departments of Chemistry, University of Glasgow, Glasgow G12 8QQ, Great Britain, and University of Western Ontario, London, Ontario Canada N6A 5B7

Received June 19, 1984

Synthetic routes to binuclear complexes [$Pt_2Me_4(\mu$-$R_2PCH_2PR_2)_2$] (**1**, R = Me; **2**, R = Ph; **3**, R = Et) and to the mononuclear complexes [$PtMe_2(R_2PCH_2PR_2)$] (**4**, R = Ph; **5**, R = *i*-Pr) have been developed. The structures and conformations of the binuclear complexes have been studied in solution by variable-temperature ^1H and ^{31}P NMR spectroscopy. The molecular structures of **1** and **2**, determined by X-ray diffraction techniques, each contain two *cis*-$PtMe_2$ fragments held together by two bridging $R_2PCH_2PR_2$ ligands. The approximate molecular symmetry is C_{2h} in **1** and C_2 in **2**, and the eight-membered $Pt_2P_4C_2$ dimetallacycles adopt twist-chair and twist-boat conformations, respectively. In **1** the local environments of the platinum atoms are sterically more open than in **2**, where the phenyl substituents may hinder access of reagents to the metal centers. Crystals of **1** are monoclinic of space group $P2_1/a$ with a = 16.634 (4) Å, b = 11.112 (3) Å, c = 12.469 (3) Å, β = 103.40 (2)°, and Z = 4. Crystals of **2** are monoclinic of space group $P2_1/c$ with a = 13.957 (7) Å, b = 17.218 (5) Å, c = 21.649 (5) Å, β = 106.45 (3)°, and Z = 4. Least-squares refinement of the structural model of **1** defined by 181 parameters converged at a conventional R index on F of 0.043 for 3646 reflections with $I \geq 3\sigma(I)$. For **2**, the structural model involved 175 parameters and the final value of the R factor based on F was 0.068 for 3818 reflections. It is concluded that increasing steric bulk of substituents R (i) stabilizes the mononuclear with respect to the binuclear complex, (ii) is primarily responsible for determining the ground-state conformations of the binuclear complexes and the activation energies for fluxionality, and (iii) greatly decreases the reactivity of the complexes, and particularly the binuclear ones, toward oxidative addition reactions.

Introduction

In the development of the chemistry of binuclear complexes, it is often desirable to lock together two metal centers using bridging ligands.[2,3] Di(tertiary phosphines) are particularly useful for this purpose, but there is much to be learned about the factors that influence whether such ligands will bridge or chelate.[4–7] For example, ligands

(1) (a) University of Glasgow. (b) University of Western Ontario.

(2) Balch, A. L. In "Homogeneous Catalysis with Metal Phosphine Complexes"; Pignolet, L., Ed.; Plenum Press: New York, 1983.
(3) Puddephatt, R. J. *Chem. Soc. Rev.* **1983**, 99.

0276-7333/84/2303-1637$01.50/0

$R_2P(CH_2)_nPR_2$, P⌒P, with platinum(II) can give any of the complexes A–D. Shaw argued that, for n = 5–10, bulky substituents, R, stabilize the chelate B with respect to the trans dimer D as a result of conformational and entropy effects (the Thorpe–Ingold effect),[5] but this interpretation has been questioned.[7] There is no doubt that, for n = 5–16, the relative stabilities of A vs. C or B vs. D are dependent on n.[5-7]

In complexes of $Ph_2PCH_2PPh_2$, dppm, isomer A is most stable when X = Cl but D is most stable when X = C≡CR.[8,9] Isomer B is, of course, impossible in this case, and the formation of D, X = C≡CR, is dictated by the preference of alkynyl groups to be mutually trans.[9] The factors influencing the relative stabilities of A and C are more complex. First, when dppm chelates as in A, there is angle strain since the PPtP and PCP angles are constrained to ~70° and ~95° compared to the normal bond angles of 90° and 109°, respectively;[10] this angle strain would be absent or at least much less in the dimer C. However, in C much greater steric hindrance between phenyl substituents is expected compared to A, in which the phenyl groups are directed away from each other.[10] Entropic effects also favor A over C. We therefore predicted that the relative stabilities of A and C when P⌒P = $R_2PCH_2PR_2$ should be largely dependent on the bulk of R, with bulky R groups favoring A and small R groups favoring C.[2]

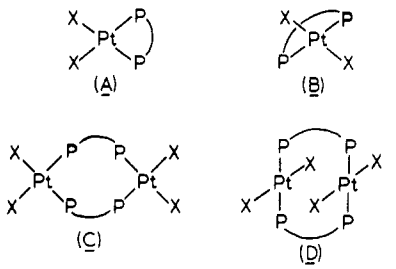

This article reports a systematic study aimed at testing the above prediction. We have used X = Me, in order to ensure that the cis stereochemistry at platinum(II) is maintained. Preliminary accounts of parts of this work have been published,[11,12] and we note that the effect of the bulk of R on the relative stabilities of A and C and on the conformation of isomer C may have relevance to amidate-bridged diplatinum(II) complexes, which are of biochemical interest.[13]

Scheme I

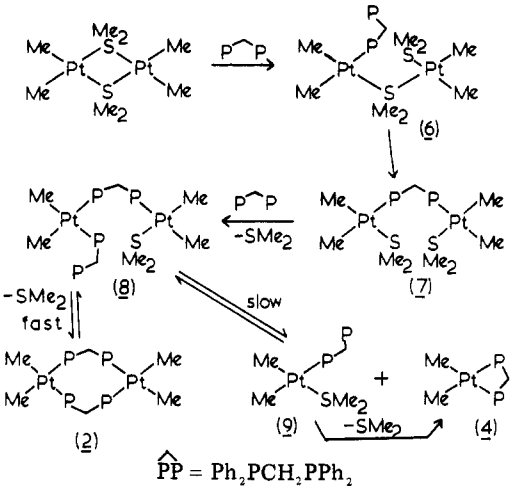

Results and Discussion

Synthesis of Complexes. Two methods were used to prepare the dimethylplatinum derivatives. Reaction of mononuclear $[PtCl_2(R_2PCH_2PR_2)]$ with methyllithium gave mononuclear $[PtMe_2(R_2PCH_2PR_2)]$, structure A, when R = Ph[14] or *i*-Pr, but binuclear *cis*-$[Pt_2Me_4(\mu\text{-}R_2PCH_2PR_2)_2]$, structure C, when R = Me or Et. Reaction of $[Pt_2Me_4(\mu\text{-}SMe_2)_2]$ with $R_2PCH_2PR_2$ gave mononuclear $[PtMe_2(R_2PCH_2PR_2)]$ only when R = *i*-Pr and binuclear *cis*-$[Pt_2Me_4(\mu\text{-}R_2PCH_2PR_2)_2]$ when R = Me, Et, or Ph, in all cases with displacement of Me_2S. Reaction of the oligomeric form of $[\{PtCl_2(Me_2PCH_2PMe_2)\}_n]$ with methyllithium also gave *cis*-$[Pt_2Me_4(\mu\text{-}Me_2PCH_2PMe_2)_2]$. The isolated complexes are therefore **1–5**.

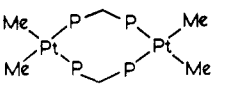

1, P⌒P = $Me_2PCH_2PMe_2$ = dmpm
2, P⌒P = $Ph_2PCH_2PPh_2$ = dppm
3, P⌒P = $Et_2PCH_2PEt_2$ = depm

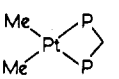

4, P⌒P = dppm
5, P⌒P = *i*-Pr_2PCH_2P-*i*-Pr_2 = dippm

Only when R = Ph, was it possible to isolate both a mononuclear form, **4**, and a binuclear form, **2**. Samples of **2** and **4** in benzene-d_6 did not interconvert, as monitored by ^1H NMR spectroscopy, even on heating to 60 °C for several days. However, in the presence of catalytic amounts of Me_2S or dppm in benzene-d_6 solution at 60 °C, binuclear **2** slowly but quantitatively converted to the monomer **4**. A solution of **4** was unchanged under these conditions. Hence, the monomer **4** is the thermodynam-

(4) (a) Bachechi, F.; Zambonelli, L.; Venanzi, L. M. *Helv. Chim. Acta* **1977**, *60*, 2815. (b) Reed, F. J. S.; Venanzi, L. M. *Helv. Chim. Acta* **1977**, *60*, 2804. (c) DeStefano, N. J.; Johnson, D. K.; Venanzi, L. M. *Helv. Chim. Acta* **1976**, *59*, 2683. (d) DeStefano, N. J.; Johnson, D. K.; Lane, R. M.; Venanzi, L. M. *Helv. Chim. Acta* **1976**, *59*, 2674.

(5) (a) Shaw, B. L. *J. Am. Chem. Soc.* **1975**, *97*, 3856. (b) Shaw, B. L. *Adv. Chem. Ser.*, **1982**, *No. 196*, 101. (c) Crocker, C.; Errington, R. J.; Markham, R.; Moulton, C. J.; Odell, K. J.; Shaw, B. L. *J. Am. Chem. Soc.* **1980**, *102*, 4373. (d) Al-Salem, N. A.; Empsall, H. D.; Markham, R.; Shaw, B. L.; Weeks, B. *J. Chem. Soc., Dalton Trans.* **1979**, 1972. (e) Pryde, A.; Shaw, B. L.; Weeks, B. *J. Chem. Soc., Dalton Trans.* **1976**, 322. (f) Shaw, B. L. *J. Organomet. Chem.* **1980**, *200*, 307.

(6) (a) Alcock, N. W.; Brown, J. M.; Jeffery, J. C. *J. Chem. Soc., Dalton Trans.* **1976**, 583; **1977**, 888.

(7) (a) Hill, W. E.; Taylor, J. G.; McAuliffe, C. A.; Muir, K. W.; Manojlović-Muir, L. *J. Chem. Soc., Dalton Trans.* **1982**, 833. (b) Hill, W. E.; Minahan, D. M. A.; Taylor, J. G.; McAuliffe, C. A. *J. Am. Chem. Soc.* **1982**, *104*, 6001.

(8) Hunt, C. T.; Balch, A. L. *Inorg. Chem.* **1981**, *20*, 2267.

(9) (a) Pringle, P. G.; Shaw, B. L. *J. Chem. Soc., Chem. Commun.* **1982**, 581. (b) Puddephatt, R. J.; Thomson, M. A. *J. Organomet. Chem.* **1982**, *238*, 231. (c) Langrick, C. R.; McEwan, D. M.; Pringle, P. G.; Shaw, B. L. *J. Chem. Soc., Dalton Trans.* **1983**, 2487.

(10) (a) Cowie, M.; Dwight, S. K. *Inorg. Chem.* **1979**, *18*, 1209. (b) Braterman, P. S.; Cross, R. J.; Manojlović-Muir, L.; Muir, K. W.; Young, G. B. *J. Organomet. Chem.* **1975**, *84*, C40.

(11) Puddephatt, R. J.; Thomson, M. A.; Manojlović-Muir, L.; Muir, K. W.; Frew, A. A.; Brown, M. P. *J. Chem. Soc., Chem. Commun.* **1981**, 805.

(12) Ling, S. S. M.; Puddephatt, R. J.; Manojlović-Muir, L.; Muir, K. W. *Inorg. Chim. Acta* **1983**, *77*, L95.

(13) (a) Hollis, L. S.; Lippard, S. J. *J. Am. Chem. Soc.* **1983**, *105*, 3494. (b) Faggiani, R.; Lock, C. J. L.; Pollock, R. J.; Rosenberg, B.; Turner, G. *Inorg. Chem.* **1981**, *20*, 804. (c) Faggiani, R.; Lippert, B.; Lock, C. J. L.; Speranzini, R. A. *J. Am. Chem. Soc.* **1981**, *103*, 1111. (d) Barton, J. K.; Rabinowitz, H. N.; Szalda, D. J.; Lippard, S. J. *J. Am. Chem. Soc.* **1977**, *99*, 2827.

(14) (a) Appleton, T. G.; Bennett, M. A.; Tomkins, I. B. *J. Chem. Soc., Dalton Trans.* **1976**, 439. (b) Cooper, S. J.; Brown, M. P.; Puddephatt, R. J. *Inorg. Chem.* **1981**, *20*, 1374.

Table I. Selected Interatomic Distances (Å) and Angles (deg) in $[Me_2Pt(\mu\text{-dmpm})_2PtMe_2]$ (1)[a,b]

Bond Distances			
Pt(A)-P(1A)	2.280 (3)	Pt(B)-P(1B)	2.264 (3)
Pt(A)-P(2A)	2.280 (3)	Pt(B)-P(2B)	2.275 (4)
Pt(A)-C(1A)	2.124 (12)	Pt(B)-C(1B)	2.133 (12)
Pt(A)-C(2A)	2.161 (12)	Pt(B)-C(2B)	2.202 (9)
P(1A)-C(3A)	1.846 (10)	P(1B)-C(3B′)	1.844 (13)
P(1A)-C(4A)	1.851 (16)	P(1B)-C(4B)	1.866 (13)
P(1A)-C(5A)	1.828 (13)	P(1B)-C(5B)	1.861 (14)
P(2A)-C(3A′)	1.825 (10)	P(2B)-C(3B)	1.870 (13)
P(2A)-C(6A)	1.816 (15)	P(2B)-C(6B)	1.808 (13)
P(2A)-C(7A)	1.841 (13)	P(2B)-C(7B)	1.836 (16)
Bond Angles			
P(1A)-Pt(A)-P(2A)	102.9 (2)	P(1B)-Pt(B)-P(2B)	102.7 (2)
P(1A)-Pt(A)-C(1A)	86.5 (4)	P(1B)-Pt(B)-C(1B)	87.7 (4)
P(1A)-Pt(A)-C(2A)	170.0 (4)	P(1B)-Pt(B)-C(2B)	169.9 (3)
P(2A)-Pt(A)-C(1A)	170.5 (4)	P(2B)-Pt(B)-C(1B)	169.5 (4)
P(2A)-Pt(A)-C(2A)	87.2 (4)	P(2B)-Pt(B)-C(2B)	87.3 (3)
C(1A)-Pt(A)-C(2A)	83.4 (5)	C(1B)-Pt(B)-C(2B)	82.3 (5)
Pt(A)-P(1A)-C(3A)	114.6 (4)	Pt(B)-P(1B)-C(3B′)	114.1 (5)
Pt(A)-P(1A)-C(4A)	123.5 (5)	Pt(B)-P(1B)-C(4B)	122.1 (5)
Pt(A)-P(1A)-C(5A)	114.4 (5)	Pt(B)-P(1B)-C(5B)	113.7 (5)
C(3A)-P(1A)-C(4A)	99.6 (6)	C(3B′)-P(1B)-C(4B)	102.2 (6)
C(3A)-P(1A)-C(5A)	100.6 (6)	C(3B′)-P(1B)-C(5B)	98.9 (6)
C(4A)-P(1A)-C(5A)	100.7 (7)	C(4B)-P(1B)-C(5B)	102.8 (7)
Pt(A)-P(2A)-C(3A′)	116.6 (4)	Pt(B)-P(2B)-C(3B)	115.4 (5)
Pt(A)-P(2A)-C(6A)	122.7 (4)	Pt(B)-P(2B)-C(6B)	123.9 (5)
Pt(A)-P(2A)-C(7A)	113.3 (5)	Pt(B)-P(2B)-C(7B)	112.6 (5)
C(3A′)-P(2A)-C(6A)	100.4 (6)	C(3B)-P(2B)-C(6B)	100.1 (6)
C(3A′)-P(2A)-C(7A)	99.9 (6)	C(3B)-P(2B)-C(7B)	101.9 (7)
C(6A)-P(2A)-C(7A)	100.4 (6)	C(6B)-P(2B)-C(7B)	99.8 (7)
P(1A)-C(3A)-P(2A)	115.7 (5)	P(1B)-C(3B)-P(2B)	114.4 (7)

[a] The letters A and B distinguish the two crystallographically independent molecules. [b] Primed atoms are related to the corresponding unprimed atoms by the symmetry operations $\bar{x}, 1-y, 1-z$ and $\bar{x}, \bar{y}, \bar{z}$ for A and B molecules, respectively.

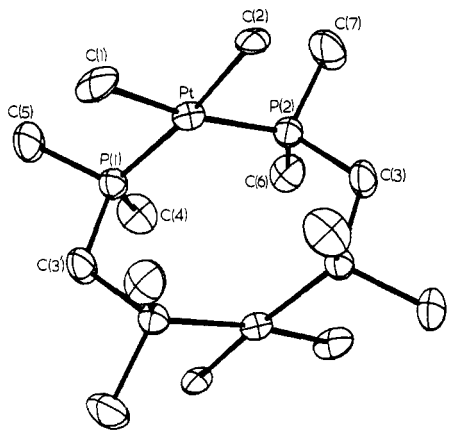

Figure 1. A perspective view of the molecular structure of $[Me_2Pt(\mu\text{-dmpm})_2PtMe_2]$ (1), showing vibrational ellipsoids with 50% probability. Hydrogen atoms are omitted. The atomic numbering scheme, which is the same for molecules A and B, is indicated.

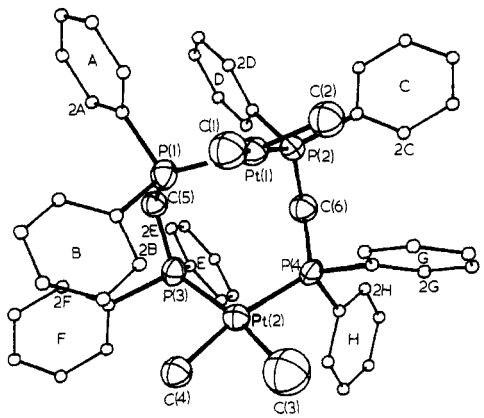

Figure 2. A perspective view of the molecular structure of $[Me_2Pt(\mu\text{-dppm})_2PtMe_2]$ (2). The phenyl group carbon atoms are shown by spheres of arbitrary radius and the remaining atoms by vibrational ellipsoids of 50% probability. In phenyl groups, A to H, the atoms are numbered in sequence, starting with Cl that is bonded to phosphorus; the direction of each sequence is indicated by labeling 2A, 2B, etc. Hydrogen atoms are omitted.

ically stable form. Solutions of **1**, **3**, and **5** gave no evidence for rearrangement under the above conditions and hence are considered to be the most stable forms. This conclusion is supported by the observation that binuclear complex **3** is formed from the mononuclear $[PtCl_2(R_2PCH_2PR_2)]$ precursor and that mononuclear **5** is formed from the binuclear precursor $[Pt_2Me_4(\mu\text{-}SMe_2)_2]$.

In the one case in which the thermodynamically unstable isomer **2** is formed, it is clear that this product must result from kinetic control and we suggest that reaction occurs according to Scheme I. The product-controlling step probably involves attack of the free phosphine in **6** at platinum, and there must be a kinetic preference for attack at the second platinum center giving **7** rather than chelation to give **4** and *cis*-$[PtMe_2(SMe_2)_2]$. The ligand-catalyzed isomerization to monomeric $[PtMe_2(Ph_2PCH_2PPh_2)]$ then occurs by a much slower sequence involving **8** and **9**. Complex **9**, L = dppm, can be generated easily by reaction of **4** with dppm.[15,16]

Determination of the Structures of 1 and 2 by X-ray Diffraction. To investigate reasons for the different reactivities of $[Me_2Pt(\mu\text{-dmpm})_2PtMe_2]$, **1**, and its dppm analogue $[Me_2Pt(\mu\text{-dppm})_2PtMe_2]$, **2**, we have determined the molecular structures of both complexes by X-ray

(15) Brown, M. P., personal communication.
(16) For platinum(II) complexes with monodentate dppm ligands which give reactions anologous to those of Scheme I see ref 9 and 17.
(17) (a) McEwan, D. M.; Pringle, P. G.; Shaw, B. L. *J. Chem. Soc., Chem. Commun.* **1982**, 859. (b) McDonald, W. S.; Pringle, P. G.; Shaw, B. L. *J. Chem. Soc., Chem. Commun.* **1982**, 861.

Table II. Selected Interatomic Distances (Å) and Angles (deg) in $[Me_2Pt(\mu\text{-dppm})_2PtMe_2]$ (2)

Bond Distances			
Pt(1)-P(1)	2.299 (9)	Pt(2)-P(3)	2.300 (8)
Pt(1)-P(2)	2.294 (8)	Pt(2)-P(4)	2.304 (8)
Pt(1)-C(1)	2.09 (4)	Pt(2)-C(3)	2.14 (6)
Pt(1)-C(2)	2.08 (4)	Pt(2)-C(4)	2.05 (4)
P(1)-C(5)	1.84 (3)	P(3)-C(5)	1.84 (3)
P(1)-C(1A)	1.83 (4)	P(3)-C(1E)	1.81 (4)
P(1)-C(1B)	1.84 (4)	P(3)-C(1F)	1.86 (4)
P(2)-C(6)	1.90 (4)	P(4)-C(6)	1.86 (3)
P(2)-C(1C)	1.83 (4)	P(4)-C(1G)	1.82 (3)
P(2)-C(1D)	1.86 (4)	P(4)-C(1H)	1.87 (3)
Bond Angles			
P(1)-Pt(1)-P(2)	97.5 (3)	P(3)-Pt(2)-P(4)	98.4 (3)
P(1)-Pt(1)-C(1)	92.8 (10)	P(3)-Pt(2)-C(3)	170.3 (15)
P(1)-Pt(1)-C(2)	166.0 (10)	P(3)-Pt(2)-C(4)	90.4 (9)
P(2)-Pt(1)-C(1)	169.7 (10)	P(4)-Pt(2)-C(3)	91.3 (14)
P(2)-Pt(1)-C(2)	94.7 (10)	P(4)-Pt(2)-C(4)	168.9 (9)
C(1)-Pt(1)-C(2)	75.0 (14)	C(3)-Pt(2)-C(4)	79.9 (17)
Pt(1)-P(1)-C(5)	122.7 (10)	Pt(2)-P(3)-C(5)	120.6 (10)
Pt(1)-P(1)-C(1A)	108.3 (11)	Pt(2)-P(3)-C(1E)	115.6 (11)
Pt(1)-P(1)-C(1B)	116.2 (11)	Pt(2)-P(3)-C(1F)	114.5 (11)
C(5)-P(1)-C(1A)	101.3 (14)	C(5)-P(3)-C(1E)	101.1 (13)
C(5)-P(1)-C(1B)	105.0 (14)	C(5)-P(3)-C(1F)	102.9 (14)
C(1A)-P(1)-C(1B)	99.9 (15)	C(1E)-P(3)-C(1F)	99.1 (14)
Pt(1)-P(2)-C(6)	121.5 (10)	Pt(2)-P(4)-C(6)	121.0 (10)
Pt(1)-P(2)-C(1C)	118.5 (10)	Pt(2)-P(4)-C(1G)	118.3 (9)
Pt(1)-P(2)-C(1D)	113.1 (10)	Pt(2)-P(4)-C(1H)	108.2 (10)
C(6)-P(2)-C(1C)	101.1 (13)	C(6)-P(4)-C(1G)	104.1 (13)
C(6)-P(2)-C(1D)	100.1 (14)	C(6)-P(4)-C(1H)	101.4 (13)
C(1C)-P(2)-C(1D)	98.8 (14)	C(1G)-P(4)-C(1H)	100.8 (13)
P(1)-C(5)-P(3)	119.9 (15)	P(2)-C(6)-P(4)	117.1 (16)

diffraction techniques. In the crystal structure of **1** the molecules can be divided into two groups, 1A and 1B (Tables I and V), which are crystallographically independent from each other but structurally practically identical within the limits of experimental errors.

The molecular structures of the two complexes, characterized by bond lengths and angles listed in Tables I and II, are closely similar to one another (Figures 1 and 2). Each contains two *cis*-$PtMe_2$ fragments, spanned by two bridging $R_2PCH_2PR_2$ ligands to form an eight-membered ring in which both metal centers lie in square-planar local environments. The main difference between the two structures lies in the conformations of their $Pt_2P_4C_2$ dimetallacycles and in the associated molecular symmetries. In **1**, 1A and 1B molecules straddle crystallographic centers of inversion but approximate to C_{2h} symmetry, the noncrystallographic diad axis passing through the two methylenic carbon atoms C(3) and C(3′). Molecules of **2**, on the other hand, show approximate C_2 symmetry, with the twofold axis normal to the plane of the four phosphorus atoms and bisecting the Pt···Pt distance.

Selected structural features of **1** and **2**, compared in Table III, show that the Pt–C and P–C bond lengths are equal in the two complexes. The Pt–P bonds are somewhat shorter in **1** than in **2**, but this is compatible with different steric demands of the Me and Ph substituents of the $R_2PCH_2PR_2$ ligands. In both complexes the bond angles within the eight-membered $Pt_2P_4C_2$ rings are substantiably more obtuse than the idealised values of 90° at platinum and 109.5° at phosphorus and carbon atoms. The distortions of the P–Pt–P angles in **2** are smaller than in **1**; this, however, is compensated by larger openings of the Pt–P–C and P–C–P ring angles, so that in **2** the dppm ligands display exceptionally large P···P bite distances [3.183 (11) and 3.203 (11) Å]. These are some 0.3 Å longer than the corresponding P···P distances in dppm-bridged diplatinum complexes in which the metal atoms are directly linked by Pt–Pt σ bonds.[18] They are also longer than the P···P bite distances of the dmpm ligands in **1** [3.108 (4) and 3.122 (4) Å].

Table III. Mean Dimensions (Å and deg) of $[Me_2Pt(\mu\text{-L})_2PtMe_2]$ Molecules

	1 (L = dmpm)	**2** (L = dppm)
point group[a]	C_{2h}	C_2
Pt-P	2.275 (4)	2.299 (2)
Pt-C	2.16 (2)	2.09 (2)
P-C	1.841 (6)	1.85 (1)
P-Pt-P	102.8 (2)	98.0 (5)
Pt-P-CH_2	115.2 (6)	121.5 (5)
P-C-P	115.1 (7)	118.5 (14)
C-Pt-C	82.9 (6)	77 (3)
ω_1[b]	111 (1)	22 (1)
ω_2	−44 (1)	73 (1)

[a] Assumed in averaging. Esd's are larger of range and pooled individual estimates. [b] The two types of ring skeleton torsion angle are defined by the following diagrams:

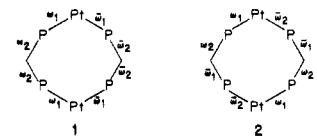

1 2

Torsion angle ranges: $|\omega_1|$ = 109.2 (4)-113.9 (5) for **1** and 18.9 (12)-24.2 (11) for **2**.

Molecular overcrowding is severe in both complexes. It is evident not only from the deformations of the bond angles (Table III) but also from the presence of some very short intramolecular nonbonding distances. In **1** the methyl groups attached to platinum atoms are in close

(18) (a) Manojlović-Muir, L.; Muir, K. W.; Solomun, T. *Acta Crystallogr., Sect. B* **1979**, *B35*, 1237. (b) Manojlović-Muir, L.; Muir, K. W.; Solomun, T. *J. Organomet. Chem.* **1979**, *179*, 479. (c) Brown, M. P.; Cooper, S. J.; Frew, A. A.; Manojlović-Muir, L.; Muir, K. W.; Puddephatt, R. J.; Seddon, K. R.; Thomson, M. A. *Inorg. Chem.* **1981**, *20*, 1500. (d) Manojlović-Muir, L.; Muir, K. W. *J. Organomet. Chem.* **1981**, *219*, 129. (e) Fisher, J. R.; Mills, A. J.; Summer, S.; Brown, M. P.; Thomson, M. A.; Puddephatt, R. J.; Frew, A. A.; Manojlović-Muir, L.; Muir, K. W. *Organometallics* **1982**, *1*, 1421.

contact with equatorial substituents at phosphorus [C(1)···C(5) and C(2)···C(7) = 3.25 (2)–3.37 (2) Å, in A and B molecules], and the axial methyl groups C(4) and C(6) are separated by 3.22 (2) and 3.26 (2) Å only. The C(4)···C(6) distances would have been even shorter if it were not for the opening of Pt–P–C(axial) angles to 122.1 (5)–123.9 (5)° (Table I). These angles are substantially larger than the Pt–P–C(equatorial) angles Pt–P–C(5) and Pt–P–C(7) = 112.6 (5)–114.4 (5)°. In **2** each methyl ligand is in close contact with a phenyl group attached to the cis phosphorus [C(1)···C(1B) = 3.36 (5), C(2)···C(2C) = 3.28 (5), C(3)···C(6G) = 3.41 (6), and C(4)···C(1F) = 3.12 (4) Å] and the phenyl ring pairs A/D, B/F, C/G, D/E, and E/H (Figure 2) are separated from one another by C···C distances of 3.42 (5)–3.54 (5) Å. The substantial steric congestion found in these complexes may be responsible for the closure of the *cis*-C–Pt–C angles to 82.9 (6)° in **1** and 77 (3)° in **2**. Such acute angles subtended by monodentate terminal ligands at divalent platinum are unusual; they are however comparable with L–Pt(II)–L angles in some four-membered chelate rings such as in $[PtPh_2(dppm)]$, for example, (P–Pt–P = 73°).[10b]

The intramolecular Pt···Pt separations 4.276 (1) and 4.198 (1) Å in **1** and 4.361 (2) Å in **2** are much too long to permit any direct bonding interactions between the metal atoms. Steric effects apart, fairly free rotation would then be expected about all eight bonds defining the skeleton of each $Pt_2P_4C_2$ dimetallacycle. Conformations of the eight-membered rings in **1** and **2** may thus be compared with those of cyclooctane and its derivatives, which have been extensively studied by both experimental and theoretical techniques.[19,20] The C_{2h} molecular symmetry of **1** implies that, ignoring signs, the torsion angles about all four Pt–P bonds are equal to each other, as are those about the four P–C bonds. Indeed, the observed individual torsion angles all lie within 3° of their mean values of 111° about the Pt–P and −44° about the P–C bonds (Table III). These mean values are comparable with those of 109.3 and −37.3° characteristic of the C_{2h} twist-chair (or long-chair) conformation of cyclooctane.[20] In **2** the C_2 molecular symmetry suggests that there should be four independent torsion angles within the ring. The observed torsion angles however cluster closely about two values, 22 and 73°. These values and their distribution round the ring (Table III) indicate that the conformation of the $Pt_2P_4C_2$ dimetallacycle in **2** is a distorted form of the S_4 twist-boat (or twist-saddle) conformation of cyclooctane, which is characterized by two torsion angles, 37.6 and 64.9°. In cyclooctane itself the twist-boat is a stable conformation, while the twist-chair is highly strained and considered of interest only as a possible transition state in interconversion of other, more stable conformers. Strain energy calculations, such as are available for substituted cyclooctanes, do not suggest that the pattern of methyl group substitution analogous to that found in **1** should improve the stability of the twist-chair, relative to the stabilities of similarly substituted forms of other conformers.[20]

The steric crowding discussed above and the space-filling molecular models shown in Figures 3 and 4 indicate that it is unlikely that the bulk of the phenyl substituents of the $R_2PCH_2PR_2$ ligands could be tolerated in the C_{2h} twist-chair conformation of the $Pt_2P_4C_2$ ring. The adoption of such a conformation by the $Me_2PCH_2PMe_2$ complex **1** concentrates the phosphine substituents close to the coordination plane of each platinum atom, leaving the metal

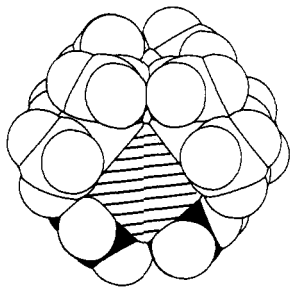

Figure 3. A space-filling model of a $[Me_2Pt(\mu\text{-dmpm})_2PtMe_2]$ molecule, viewed along the normal to a platinum atom coordination plane. Here, and in Figure 4, the Pt atom is cross-hatched, the methyl C atoms attached to Pt are black, and all H atoms are included in calculated positions.

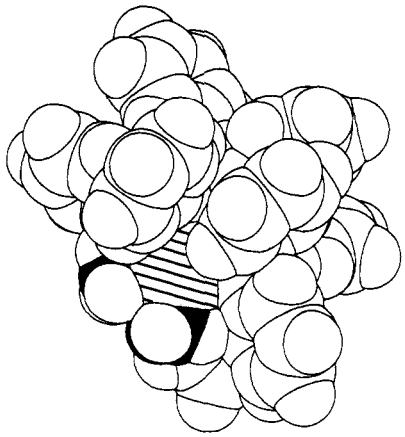

Figure 4. A space-filling model of a $[Me_2Pt(\mu\text{-dppm})_2PtMe_2]$ molecule, viewed along the normal to the coordination plane of a platinum atom.

centers in exposed environments and thus open to attack by reagents (Figure 3). The twist-boat conformation of the $Ph_2PCH_2PPh_2$ complex **2** enables the phenyl groups to provide considerably more shielded local environments for the platinum atoms (Figure 4) and thus to hinder access of reagents to the metal centers. The molecular structures of **1** and **2** therefore demonstrate that the steric properties of the substituents of the $R_2PCH_2PR_2$ ligands may be of major importance in determining reactivity of these complexes.

Indeed, it has been found that **1** and **2** display different reactivities with reagents such as I_2 and MeI, for example. The dmpm dimer **1** is reactive in oxidative addition with both substances.[12] With **2** such reactions are precluded by substantially increased steric requirements of the dppm ligands. Instead, **2** undergoes electrophilic cleavage of a methyl group with I_2 and fails to react with MeI.[11]

Characterization of Complexes in Solution. The NMR spectra of the complexes **1**–**5** give a clear distinction between the mononuclear and binuclear structures. In the $^{31}P\{^1H\}$ NMR spectra the mononuclear complexes **4** and **5** give a singlet, with singlet satellites of one-fourth intensity due to coupling with ^{195}Pt. However, in the dimers **1**–**3** the ^{195}Pt satellites are complex as shown in Figure 5. Analysis of the fine structure gives the coupling constants $^2J(PCP)$ and $^4J(PPtPCP)$ but not $^2J(PPtP)$ (Experimental Section).[21,22]

(19) Anet, F. A. L. *Top. Curr. Chem.* **1974**, *45*, 169 and references therein.

(20) Hendrickson, J. B. *J. Am. Chem. Soc.* **1967**, *89*, 7043.

(21) Brown, M. P.; Puddephatt, R. J.; Rashidi, M.; Seddon, K. R. *J. Chem. Soc., Dalton Trans.* **1977**, 951.

(22) The absence of a central peak in the ^{195}Pt satellite spectra is due to the low value of $^2J(PPtP)$ in cis complexes. In related complexes with trans stereochemistry analyzed previously[21] a central peak is observed since $^2J(PPtP)$ is large in trans complexes.[23] This is a useful criterion for distinguishing between cis and trans stereochemistries in $Pt_2(\mu\text{-}R_2PCH_2PR_2)_2$ complexes.

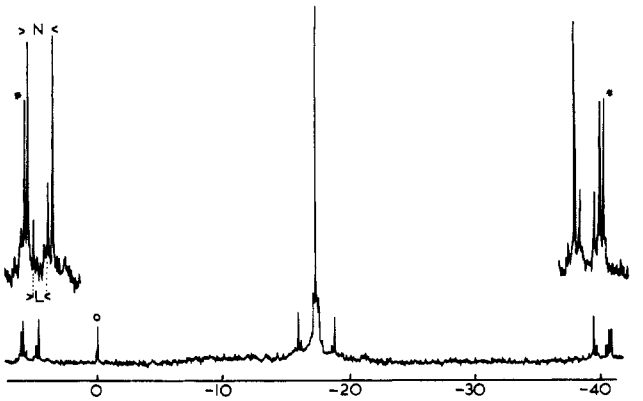

Figure 5. $^{31}P\{^1H\}$ NMR spectrum (40.5 MHz) of complex **1**. Peak marked 0 is due to reference $(MeO)_3PO$. The inset shows an expansion of the ^{195}Pt satellites: parameters $N = {}^2J(P^aP^b) + {}^3J(P^aP^{b\prime})$ and $L = {}^2J(P^aP^b) - {}^3J(P^aP^{b\prime})$. Peaks marked asterisk are due to the $^{195}Pt_2$ isotopomer and are separated by $^1J(PtP) + {}^3J(PtP)$.

In the ^1H NMR spectra of **4** and **5** the resonance due to the CH_2P_2 protons appears as a 1:2:1 triplet due to coupling to ^{31}P with one-fourth intensity satellites due to coupling to ^{195}Pt. However for the dimers **1–3** the CH_2P_2 signal appeared as a quintet with intensities close to 1:8:18:8:1 due to coupling to ^{195}Pt as expected for a group bridging between two platinum atoms[21] (Figure 6) and coupling to ^{31}P was not resolved. The very different geminal coupling constants $^2J(PCH)$ between monomers **4** and **5** [with $^2J(PH) \approx 3$ Hz] and dimers **1** to **3** [with $^2J(PH)$ small] is presumably due to the great difference in PCP bond angles discussed earlier.

A more subtle problem concerns the conformation of the dimers **1–3** in solution. The structure for **1**, determined by X-ray diffraction in the solid state, has approximately C_{2h} symmetry and all *Me*Pt, *P*Pt and CH_2P_2 atoms are in virtually identical environments. However, the two methyl groups bound to a given phosphorus atom are nonequivalent, and hence two MeP signals should be observed. This is the case at low temperature ($\Delta\nu = 323$ Hz, $T_c = 20$ °C at 400 MHz) in the ^1H NMR spectrum, but at room temperature only one broad peak is observed (Figure 6). This is fully consistent with the static structure being as in Figure 1, but with inversion of the twist-chair being rapid on the NMR time scale above room temperature. Analysis gives $\Delta G^\ddagger \approx 56$ kJ mol^{-1} for the inversion process.[23] No splitting of resonances due to *Me*Pt, CH_2P_2 or PtP_2 resonances occurred at low temperature.

The variable-temperature NMR spectra for **2** were more complex. In the structure of Figure 2 with approximately C_2 symmetry, the two methyl groups and two phosphorus atoms bound to a single platinum center are nonequivalent and so are the two protons in each CH_2P_2 group. At low temperature two *Me*Pt, two CH_2P, and two ^{31}P resonances are observed as expected for this structure (Figure 7). However, as the temperature was raised, the two *Me*Pt ($\Delta\nu = 98$ Hz at 100 MHz, $T_c \approx 0$ °C) and ^{31}P ($\Delta\nu = 179$ Hz at 40.5 MHz, $T_c \approx 10$ °C) resonances coalesced first, giving $\Delta G^\ddagger = 54.7 \pm 0.4$ kJ mol^{-1}, and the two $CH^AH^BP_2$ resonances coalesced at a higher temperature ($\Delta\nu = 131$ Hz, $T_c \approx 35$ °C), giving a correspondingly higher $\Delta G^\ddagger = 61$ kJ mol^{-1}. This is fully consistent with the static solution structure having C_2 symmetry, displaying the S_4 twist-boat conformation of the $Pt_2P_4C_2$ ring, as in Figure 2. A simple twisting motion going through a boat–boat (or saddle) intermediate can lead to equivalence of the Me_2Pt and P_2Pt groups as shown in eq 1 (Newman projection down

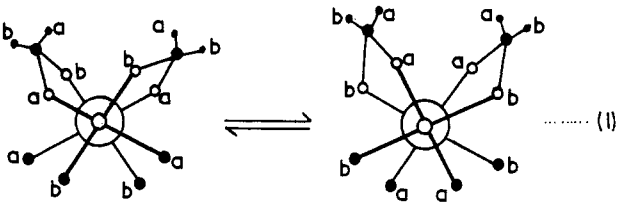

PtPt axis, a and b represent nonequivalent atoms), but this does not lead to equivalence of the CH_2P_2 protons. A second dynamic process involving inversion of the ring is necessary for equivalence of the CH_2P_2 protons and this requires a higher activation energy.

Although the NMR data above are fully consistent with the solution structure being the same as the solid-state structure for **2**, they do not prove this conclusively. For example the boat–chair conformation **10** which is the most

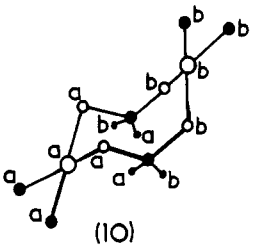

stable conformation in cyclooctane,[19,20] might give very similar NMR behavior. However, in **10** the two Pt centers are nonequivalent but we observe only one resonance in the low-temperature $^{195}Pt\{^1H\}$ NMR spectrum, so that this conformation is not possible.[24] The data are, of course, also inconsistent with the twist-chair configuration found for **1**.

The energetics of interconversions of cyclooctane conformations have been studied in detail.[19,20,25,26] According to calculations for cyclooctane, the inversion of the twist-chair conformation found for **1** would involve a sequence (T = twist, C = chair, B = boat) TC ⇌ C ⇌ TBC ⇌ TCC ⇌ B, while the inversion of the TB_4 conformation of **2** would involve a sequence TB_4 ⇌ B ⇌ TCC ⇌ TBC ⇌ C. The twisting motion for **2** involves the TB_4 ⇌ BB transformation that is expected to have a very low activation energy for cyclooctane[25,26] but has an activation energy of ~55 kJ mol^{-1} for **2** as a result of steric interactions of the phenyl substituents. If the above mechanisms are followed, the intermediates involved in ring inversion for **1** and **2** will be the same, with the inversion step involving a boat–chair interconversion in each case.

The conformation of **3** in solution is less certain than for **1** and **2**. In the ^1H NMR spectrum the only resonance that splits at low temperature is that due to the CH_3 protons of the ethyl groups. The coalescence temperature was ~0 °C with $\Delta\nu = 7$ Hz at 100 MHz, giving $\Delta G^\ddagger \approx 60$ kJ mol^{-1}. It is probable that the conformation of this complex is close to the C_{2h} conformation adopted by **1**, and

(23) Approximate values for $\Delta G^\ddagger$ were calculated by using the Eyring approximation: $\Delta G^\ddagger = RT_c \ln (2^{1/2}k_BT_c/k\pi\Delta\nu)$, where T_c = coalescence temperature (K) and $\Delta\nu$ = frequency difference (Hz) in the slow-exchange limit.

(24) Selective decoupling experiments confirm this conclusion. Thus selective decoupling at each ^{31}P resonance frequency caused partial collapse of both MePt resonances at −50 °C. For **10**, complete collapse of only one MePt resonance would be expected in each such experiment. The result proves that the two Me groups and ^{31}P groups bound to each Pt center are nonequivalent.

(25) Hendrickson, J. B. *J. Am. Chem. Soc.* **1967**, *89*, 7047.
(26) Anet, F. A. L.; St. Jacques, M. *J. Am. Chem. Soc.* **1966**, *88*, 2585, 2586.

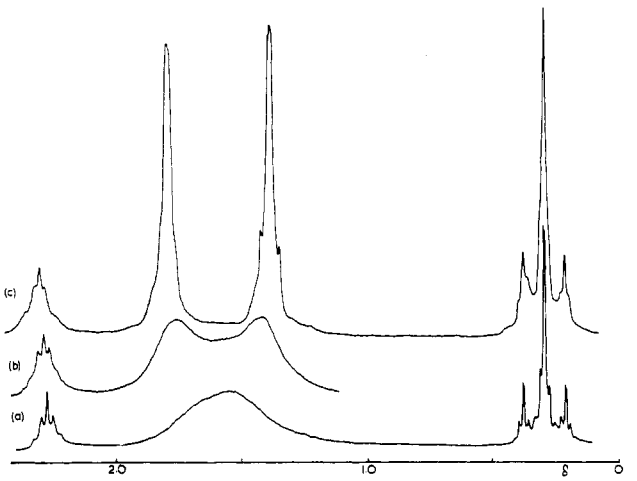

Figure 6. ^1H NMR spectra (400 MHz) of complex 1: (a) at 20 °C, (b) at 10 °C, and (c) at −70 °C.

Table IV. Crystallographic Data for the Complexes $[Me_2Pt(\mu\text{-}R_2PCH_2PR_2)_2PtMe_2]$

	1 (R = Me)	2 (R = Ph)
empirical formula	$C_{14}H_{40}P_4Pt_2$	$C_{54}H_{56}P_4Pt_2$
fw	722.55	1219.12
space group	$P2_1/a$	$P2_1/c$
a, Å	16.634 (4)	13.957 (7)
b, Å	11.112 (3)	17.218 (5)
c, Å	12.469 (3)	21.649 (5)
β, deg	103.40 (2)	106.45 (3)
V, Å^3	2242	4990
Z	4	4
D(calcd), g cm^{-3}	2.141	1.623
D(obsd), g cm^{-3}		1.65
μ(Mo Kα), cm^{-1}	128.7	58.2
F(000)	1360	2384
θ(Mo Kα)range, deg	2-27	2-25
independent observns	3646	3818
refined parameters	181	175
R	0.043	0.068
R_w	0.055	0.089

the increased activation energy compared to 1 is due to the increased steric hindrance for the larger ethyl substituents.

Conclusions

This work has demonstrated that the bulk of the substituents R in the ligands $R_2PCH_2PR_2$ has a significant effect on the stability of mononuclear $[PtMe_2(R_2PCH_2PR_2)]$ vs. dinuclear $[Pt_2Me_4(\mu\text{-}R_2PCH_2PR_2)_2]$ and on the conformations of the dinuclear forms. In particular the following trends emerge:

1. For the smaller groups R = Me or Et the binuclear structure is more stable and the mononuclear form could not be prepared. For the larger R = Ph, both isomers could be isolated, but the mononuclear form was more stable, and, with the largest group R = *i*-Pr, only the mononuclear form could be isolated. This trend is expected since steric effects are much greater in the binuclear molecules, as demonstrated by the structures of Figures 1–4. Steric effects in the binuclear 2 are particularly severe and would be even worse in the corresponding complex with R = *i*-Pr. It can be concluded that the eight-membered ring of the binuclear species is less strained than the four-membered ring of the mononuclear ones, and hence for small substituents R the binuclear forms are more stable. However, as the bulk of R increases, this effect is offset by the greater steric interactions in the binuclear forms and so, for large R groups, the mononuclear structure is favored.

2. The conformation of the dimer is also affected by steric effects and results in different ground-state conformations for complexes 1 and 2. The conformations determined by X-ray diffraction studies in the solid state for 1 and 2 are also the most stable conformations in solutions, as deduced from the NMR studies. The relatively high activation energies for interconversion of conformational isomers is again due to steric constraints.

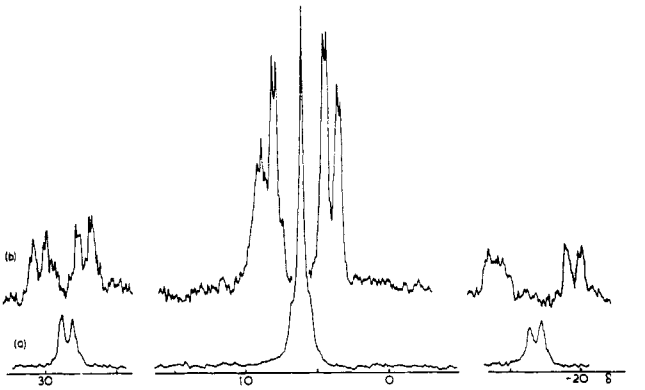

Figure 7. $^{31}P\{^1H\}$ NMR spectra (40.5 MHz) of complex 2: (a) at 50 °C and (b) at −50 °C.

Table V. Atomic Coordinates and Equivalent Isotropic Thermal Parameters for $[Me_2Pt(\mu\text{-dmpm})_2PtMe_2]$ (1)

atom	x/a	y/b	z/c	U,[a] Å^2
Pt(A)	0.03023 (2)	0.33160 (4)	0.43632 (3)	0.0315 (3)
Pt(B)	−0.08009 (2)	0.13976 (4)	0.02027 (3)	0.0332 (3)
P(1A)	0.13063 (15)	0.47477 (28)	0.45396 (21)	0.036 (2)
P(2A)	−0.08349 (15)	0.42752 (27)	0.33523 (21)	0.034 (2)
P(1B)	0.05514 (16)	0.18498 (27)	0.08573 (23)	0.037 (2)
P(2B)	−0.09407 (16)	−0.03567 (28)	0.10821 (23)	0.040 (2)
C(1A)	0.1238 (7)	0.2161 (10)	0.5257 (10)	0.047 (8)
C(2A)	−0.0480 (7)	0.1762 (10)	0.4359 (12)	0.051 (9)
C(3A)	0.1652 (6)	0.5375 (10)	0.5941 (7)	0.037 (8)
C(4A)	0.1182 (8)	0.6159 (14)	0.3730 (11)	0.063 (10)
C(5A)	0.2287 (7)	0.4199 (14)	0.4305 (11)	0.063 (11)
C(6A)	−0.0773 (7)	0.5690 (13)	0.2648 (11)	0.060 (10)
C(7A)	−0.1423 (7)	0.3362 (13)	0.2204 (10)	0.060 (12)
C(1B)	−0.0909 (8)	0.3023 (11)	−0.0730 (9)	0.050 (8)
C(2B)	−0.2115 (5)	0.1223 (10)	−0.0636 (9)	0.035 (6)
C(3B)	−0.1181 (8)	−0.1712 (11)	0.0174 (11)	0.055 (8)
C(4B)	0.1204 (7)	0.1064 (13)	0.2075 (10)	0.056 (11)
C(5B)	0.0744 (8)	0.3467 (12)	0.1216 (12)	0.062 (10)
C(6B)	−0.0153 (8)	−0.0972 (12)	0.2195 (10)	0.053 (8)
C(7B)	−0.1817 (9)	−0.0329 (14)	0.1747 (13)	0.085 (12)

[a] Defined as $^1/_3(U_{11} + U_{22} + U_{33})$.

Table VI. Atomic Coordinates and Thermal Parameters for $[Me_2Pt(\mu\text{-dppm})_2PtMe_2]$ (2)

atom	x/a	y/b	z/c	U,[a] Å^2
Pt(1)	0.12452 (9)	0.01978 (7)	0.19525 (6)	0.0513 (8)
Pt(2)	0.38994 (9)	0.16589 (7)	0.23176 (6)	0.0468 (7)
P(1)	0.1740 (6)	0.0730 (5)	0.2968 (4)	0.048 (5)
P(2)	0.2480 (6)	−0.0721 (4)	0.2102 (4)	0.047 (5)
P(3)	0.4041 (6)	0.1191 (4)	0.3335 (4)	0.045 (5)
P(4)	0.4041 (6)	0.0497 (4)	0.1823 (4)	0.044 (4)
C(1)	0.004 (3)	0.095 (2)	0.165 (2)	0.073 (10)
C(2)	0.045 (2)	−0.020 (2)	0.104 (2)	0.069 (9)
C(3)	0.376 (4)	0.228 (3)	0.144 (3)	0.132 (18)
C(4)	0.394 (2)	0.278 (2)	0.265 (1)	0.058 (8)
C(5)	0.302 (2)	0.063 (2)	0.350 (1)	0.043 (7)
C(6)	0.382 (2)	−0.044 (2)	0.218 (1)	0.053 (8)
C(1A)	0.101 (2)	0.028 (2)	0.345 (1)	0.056 (8)
C(2A)	0.143 (3)	0.003 (2)	0.408 (2)	0.094 (13)
C(3A)	0.083 (3)	−0.031 (2)	0.442 (2)	0.096 (13)
C(4A)	−0.018 (3)	−0.040 (3)	0.413 (2)	0.103 (14)
C(5A)	−0.059 (3)	−0.015 (3)	0.351 (2)	0.100 (13)
C(6A)	0.000 (3)	0.018 (2)	0.317 (2)	0.086 (11)
C(1B)	0.141 (2)	0.176 (2)	0.303 (2)	0.065 (9)
C(2B)	0.161 (2)	0.229 (2)	0.261 (2)	0.065 (9)
C(3B)	0.135 (4)	0.306 (3)	0.264 (3)	0.159 (22)
C(4B)	0.089 (3)	0.329 (2)	0.309 (2)	0.090 (12)
C(5B)	0.068 (3)	0.276 (3)	0.351 (2)	0.103 (14)
C(6B)	0.094 (3)	0.199 (2)	0.349 (2)	0.081 (11)
C(1C)	0.231 (2)	−0.153 (2)	0.153 (1)	0.052 (8)
C(2C)	0.223 (3)	−0.136 (3)	0.089 (2)	0.103 (14)
C(3C)	0.200 (3)	−0.195 (2)	0.044 (2)	0.102 (14)
C(4C)	0.184 (4)	−0.269 (3)	0.062 (3)	0.134 (18)
C(5C)	0.191 (4)	−0.286 (3)	0.126 (3)	0.134 (18)
C(6C)	0.215 (4)	−0.227 (3)	0.171 (2)	0.118 (16)
C(1D)	0.265 (2)	−0.129 (2)	0.286 (1)	0.057 (8)
C(2D)	0.179 (2)	−0.149 (2)	0.301 (1)	0.057 (8)
C(3D)	0.185 (3)	−0.190 (2)	0.357 (2)	0.097 (13)
C(4D)	0.277 (3)	−0.212 (2)	0.397 (2)	0.090 (12)
C(5D)	0.363 (4)	−0.193 (3)	0.381 (3)	0.155 (21)
C(6D)	0.357 (3)	−0.151 (2)	0.325 (2)	0.071 (10)
C(1E)	0.509 (2)	0.055 (2)	0.367 (1)	0.053 (8)
C(2E)	0.507 (3)	0.000 (2)	0.413 (2)	0.075 (10)
C(3E)	0.588 (3)	−0.049 (2)	0.436 (2)	0.088 (12)
C(4E)	0.670 (3)	−0.042 (2)	0.413 (2)	0.093 (13)
C(5E)	0.672 (3)	0.013 (2)	0.367 (2)	0.082 (11)
C(6E)	0.592 (3)	0.061 (2)	0.344 (2)	0.087 (12)
C(1F)	0.431 (2)	0.194 (2)	0.398 (1)	0.057 (8)
C(2F)	0.358 (2)	0.219 (2)	0.425 (2)	0.058 (8)
C(3F)	0.377 (3)	0.280 (2)	0.468 (2)	0.075 (10)
C(4F)	0.468 (3)	0.317 (2)	0.484 (2)	0.074 (10)
C(5F)	0.541 (3)	0.292 (2)	0.456 (2)	0.075 (10)
C(6F)	0.523 (3)	0.231 (2)	0.413 (2)	0.070 (10)
C(1G)	0.339 (2)	0.039 (1)	0.097 (1)	0.041 (7)
C(2G)	0.381 (2)	0.004 (2)	0.054 (1)	0.049 (7)
C(3G)	0.328 (2)	−0.001 (2)	−0.010 (2)	0.066 (9)
C(4G)	0.233 (3)	0.029 (2)	−0.031 (2)	0.079 (11)
C(5G)	0.190 (3)	0.064 (2)	0.012 (2)	0.072 (10)
C(6G)	0.243 (3)	0.069 (2)	0.076 (2)	0.072 (10)
C(1H)	0.537 (2)	0.039 (2)	0.181 (1)	0.048 (7)
C(2H)	0.582 (2)	−0.032 (2)	0.180 (1)	0.055 (8)
C(3H)	0.683 (2)	−0.035 (2)	0.183 (2)	0.068 (9)
C(4H)	0.737 (2)	0.032 (2)	0.187 (2)	0.066 (9)
C(5H)	0.691 (3)	0.103 (2)	0.188 (2)	0.093 (12)
C(6H)	0.591 (3)	0.106 (2)	0.185 (2)	0.081 (11)

[a] For Pt and P atoms, $U = {}^1/_3(U_{11} + U_{22} + U_{33})$; for C atoms isotropic temperature factors of the form $\exp(-8\pi^2 U (\sin^2\theta)/\lambda^2)$ were used.

3. The increased steric effects in binuclear structures are also responsible for the very low reactivity toward oxidative addition of **2** compared to the mononuclear complex **4**.[11,12]

The classic work of Tolman focussed attention on the importance of steric effects on reactivity and structure of mononuclear complexes with tertiary phosphine ligands.[27] This work indicates that such effects will be of even greater significance in binuclear complexes.

Experimental Section

^{1}H NMR spectra were recorded by using Varian XL100 or Bruker WP400 spectrometers, ^{31}P NMR spectra by using Varian XL100 or XL200 spectrometers, and ^{195}Pt NMR spectra by using a Bruker WP400 spectrometer. Chemical shifts are quoted with respect to Me_4Si (^{1}H) or $(MeO)_3PO$ (^{31}P).

$[Pt_2Me_4(\mu\text{-}SMe_2)_2]$[28] and $[PtMe_2(dppm)]$,[14] were prepared as described previously. Ligands $R_2PCH_2PR_2$ (dmpm, R = Me; depm, R = Et; dippm, R = *i*-Pr) were prepared by the literature method.[29]

(27) Tolman, C. A. *Chem. Rev.* **1977**, *77*, 313.

(28) Scott, J. D. Puddephatt, R. J. *Organometallics* **1983**, *2*, 1643.

$[Pt_2Me_4(\mu\text{-dppm})_2]$. $[Pt_2Me_4(\mu\text{-}SMe_2)_2]$ (0.50 g) and dppm (0.68 g) were dissolved in dry C_6H_6 (15 mL). After 2 h at room temperature, the volume of the solution was reduced and pentane was added to precipitate the product as a white solid, which was recrystallized from CH_2Cl_2/pentane (0.72 g, 68%). NMR in CD_2Cl_2 at −50 °C: ^1H, δ 0.63 [m, $^3J(PH) = 7.5$, $^2J(PtH) = 70$ Hz, MePt], −0.35 [m, $^3J(PH) = 7.5$, $^2J(PtH) = 70$ Hz, MePt], 4.25 [m, $^2J(H^aH^b) = 13.5$, $^3J(PtH) = 28$ Hz, $CH^aH^bP_2$], 2.95 [m, $^2J(H^aH^b) = 13.5$ Hz, $CH^aH^bP_2$]; ^{31}P, δ 8.91 [m, $^1J(Pt) = 1790$ Hz, P^a], 4.49 [m, $^1J(PtP) = 1830$, $^2J(P^aP^b) = 40$, $^3J(P^aP^b) = 10$ Hz, P^b]; ^{195}Pt, δ −880 from *cis*-$[PtCl_2(SMe_2)_2]$, [*t*, $^1J(PtP) = 1800$ Hz]. Anal. Calcd for $C_{54}H_{56}P_4Pt_2$: C, 53.2; H, 4.6. Found: C, 53.0; H, 4.6.

$[Pt_2Me_4(\mu\text{-dmpm})_2]$. This was prepared in a similar way from $[Pt_2Me_4(\mu\text{-}SMe_2)_2]$ (1.13 g) and dmpm (0.59 g) in CH_2Cl_2 (50 mL) under an N_2 atmosphere: yield 1.33 g (93%). It was recrystallized from CH_2Cl_2/pentane. Anal. Calcd for $C_{14}H_{40}P_4Pt_2$: C, 23.3; H, 5.5. Found: C, 23.3; H, 5.7.

The same complex was prepared from $[PtCl_2(dmpm)]_2$ with excess methyllithium in ether–tetrahydrofuran in ~30% yield and was identified by the ^1H and ^{31}P NMR spectra in CD_2Cl_2: ^1H NMR δ 0.29 [m, $^2J(PtH) = 66$, $^3J(PH) + {}^3J(P'H) = 1.8$ Hz, MePt], 2.57 [m, $^3J(PtH) = 19$ Hz, MeP], 4.25 [m, $^3J(PtH) = 23$ Hz, CH_2P_2]; ^{31}P, δ −17.4 [m, $^1J(PtP) = 1835$, $^3J(PtP) = 65$, $^2J(P^aP^b) = 40$, $^3J(P^aP^{b\prime}) = 10$ Hz, PPt].

$[Pt_2Me_4(depm)_2]$. This complex was prepared by reaction of $[Pt_2Me_4(\mu\text{-}SMe_2)_2]$ (0.37 g) with depm (0.32 g) in CH_2Cl_2 (20 mL) under N_2: yield 0.274 g (50%); mp 205–210 °C. Anal. Calcd for $C_{22}H_{56}P_4Pt_2$: C, 31.65; H, 6.8. Found: C, 31.85; H, 6.9.

The same complex was prepared in impure form by reaction of $[PtCl_2(depm)]$ (0.200 g) in ether (10 mL) with excess MeLi (10 mL, 1.9 M solution in ether): yield 44%. NMR in CD_2Cl_2: ^1H, δ 0.24 [m, $^2J(PtH) = 66$, $^3J(PH) + {}^3J(P'H) = 1.5$ Hz, MePt], 0.85 [m, $^3J(HH) = 7$, $^3J(PH) = 5$ Hz, CH_3], 1.72 [m, CH_3CH_2], 2.06 [m, $^3J(PtH) = 18$ Hz, CH_2P_2]; ^{31}P, δ 4.54 [m, $^1J(PtP) = 1899$, $^3J(PtP) = 66$, $^2J(P^aP^b) = 40$, $^3J(P^aP^{b\prime}) = 10$ Hz, PPt].

$[PtMe_2(dippm)]$. This complex was prepared by reaction of $[Pt_2Me_4(\mu\text{-}SMe_2)_2]$ (0.26 g) with dippm (0.25 g) in CH_2Cl_2 (10 mL) under N_2, and was recrystallized from CH_2Cl_2/pentane: yield 0.30 g. Anal. Calcd for $C_{15}H_{36}P_2Pt$: C, 38.05; H, 7.6. Found: C, 38.2; H, 7.6.

The same complex was formed (69% yield) by reaction of $[PtCl_2(dippm)]$ with excess methyllithium. NMR in $CDCl_3$: ^1H, δ 0.54 [m, $^2J(PtH) = 72$, $^3J(PH) + {}^3J(P'H) = 1$ Hz, MePt], 1.20 [dd, $^3J(HH) = 7.5$, $^3J(PH) = 14$ Hz, CH_3C], 2.19 [m, $^3J(HH) = 7.5$, $^2J(PH) = 7$ Hz, Me_2CH], 2.90 [t, $^2J(PH) = 8$, $^3J(PtH) = 17$ Hz, CH_2P_2], ^{31}P, δ −19.77 [s $^1J(PtP) = 1460$ Hz, PPt].

Reaction of $[PtMe_2(dppm)]_{1or2}$ on Heating in Benzene. Small samples (ca. 3 mg) of $[PtMe_2(dppm)]$ and $[Pt_2Me_4(\mu\text{-}dppm)_2]$ were sealed into separate 5-mm NMR tubes with C_6D_6 solvent (0.5 mL). After being heated for 48 h at 60 °C, each sample gave an unchanged ^1H NMR spectrum. The procedure was repeated with pairs of samples to which a trace amount of (i) SMe_2 and (ii) dppm was added. In each case, the ^1H NMR was recorded every 12 h, and it was observed that the samples of $[Pt_2Me_4(\mu\text{-}dppm)_2]$ converted slowly and quantitatively to $[PtMe_2(dppm)]$ over a period of 48 h. No change was observed in the tubes containing $[PtMe_2(dppm)]$.

Similar reactions of $[Pt_2Me_4(dmpm)_2]$, $[Pt_2Me_4(depm)_2]$, or $[PtMe_2(dippm)]$ gave no reaction, even in the presence of SMe_2 catalyst.

X-ray Analyses of $[Me_2Pt(\mu\text{-}L)_2PtMe_2]$, L = dmpm (1) and dppm (2). Diffraction studies of 1 and 2 were carried out on crystals mounted in air, using standard experimental and computational procedures which have already been described.[18e] Pertinent details are summarized in Table IV.

(a) Data Collection and Reduction. All X-ray measurements were made with Mo radiation and an Enraf-Nonius CAD4F diffractometer equipped with a graphite monochromator. Cell dimensions were obtained from the setting angles of 25 automatically centered high-angle reflections. The space groups were determined from the observed Laue symmetries and systematic absences.

The intensities were measured from continuous $\theta/2\theta$ scans of 1.35 and 1.27° in 0 for 1 and 2, respectively. Scan speeds were adjusted to give $\sigma(I)/I < 0.02$, subject to respective time limits of 180 and 140 s. The intensities were corrected for background, *Lp* effects, variations in the intensities of standard reflections, and absorption, using the empirical method of Walker and Stuart.[30] Symmetrically equivalent reflections were averaged; for 1, $R_{internal} = 0.077$ for 1761 duplicates, and for 2, $R_{internal} = 0.061$ for 160 duplicates. The remaining calculations for each structure employed only the independent reflections for which $I \geq 3\sigma(I)$.

(b) Structure Analyses. The platinum atoms were located from Patterson functions and the remaining non-hydrogen atoms from subsequent difference syntheses. The structures were refined by full-matrix least squares, minimizing the function $\sum w(|F_o| - |F_c|)^2$. Complex, neutral atom scattering factors were used throughout.[31]

For 1, the final calculations involved adjustment of the positional and anisotropic vibrational parameters of Pt, P, and C atoms. The scattering of the hydrogen atoms was not accounted for. An adequate weighting scheme was obtained with $w = \sigma^{-2}(F)$. In the final stages of refinement of 2 the phenyl groups were constrained to $6/mmm$ symmetry (C–C = 1.38 and C–H = 1.00 Å), with hydrogen atoms riding on the adjacent carbon atoms. Anisotropic vibrational parameters were used for Pt and P atoms only. Unit weights were found satisfactory. In the final difference syntheses for each structure all values were in the range ±2.5 e Å^{-3} and maxima and minima were close to the positions of the platinum atoms.

The final values of the positional parameters of non-hydrogen atoms are presented in Tables V and VI for 1 and 2, respectively. For both compounds the final vibrational parameters and listings of the observed and calculated structure amplitudes are available.[32]

All calculations were performed on a GOULD-SEL 32/27 mini computer, using the Glasgow crystallography (GX) program system.[33]

Acknowledgment. We thank the S.L.R.C. for assistance in purchasing the computer, the University of Glasgow for a studentship (A.A.F.), NSERC (Canada) for financial support (to R.J.P.) and for the award of a scholarship (to S.S.M.L.), and Mr. D. Srokowski and Ms. G. Milne for able experimental assistance.

Registry No. 1, 88228-39-1; 2, 79870-63-6; 3, 91491-48-4; 4, 52595-90-1; 5, 91491-49-5; $[Pt_2Me_4(\mu\text{-}SMe_2)_2]$, 79870-64-7; $[PtCl_2(dmpm)]$, 88228-37-9; $[PtCl_2(depm)]$, 91491-50-8.

Supplementary Material Available: Tables VII and VIII, anisotropic vibrational parameters for 1 and 2, Table IV, hydrogen atom coordinates and vibrational parameters for 2 and Tables X and XI, final observed and calculated structure factors for 1 and 2 (44 pages). Ordering information is given on any current masthead page.

(29) Novikova, Z. S.; Prishchenko, A. A.; Lutsenko, I. F. *J. Gen. Chem. USSR (Engl. Transl.)* **1977**, *47*, 707.

(30) Walker, N.; Stuart, D. *Acta Crystallogr., Sect. A* **1983**, *A39*, 158.

(31) "International Tables for X-Ray Crystallography"; Kynoch Press: Birmingham, United Kingdom, 1974; Vol. IV, Tables 2.2B and 2.3.1.

(32) Supplementary material.

(33) Gilmore, C. J.; Mallinson, P. R.; Muir, K. W.; White, D. N. J. *Acta Crystallogr., Sect. A* **1981**, **A37**, C-340.